Further insights into the reaction ^{14}Be(CH_{2},X)^{10}He

M. D. Jones, Z. Kohley, T. Baumann, G. Christian, P. A. DeYoung, J. E. Finck, N. Frank, R. A. Haring-Kaye, A. N. Kuchera, B. Luther, S. Mosby, J. K. Smith, J. Snyder, A. Spyrou, S. L. Stephenson, and M. Thoennessen

Phys. Rev. C **91**, 044312 — Published 15 April 2015

DOI: 10.1103/PhysRevC.91.044312

Further insights into the reaction $^{14}Be(CH_2,X)^{10}He$

M.D. Jones,[1,2,*] Z. Kohley,[1,3] T. Baumann,[1] G. Christian,[1,2,†] P.A. DeYoung,[4] J.E. Finck,[5] N. Frank,[6] R.A. Haring-Kaye,[7] A.N. Kuchera,[1] B. Luther,[8] S. Mosby,[1,2,‡] J.K. Smith,[1,2,†] J. Snyder,[1,2] A. Spyrou,[1,2] S.L. Stephenson,[9] and M. Thoennessen[1,2]

[1] *National Superconducting Cyclotron Laboratory, Michigan State University, East Lansing, MI 48824, USA*
[2] *Department of Physics and Astronomy, Michigan State University, East Lansing, MI 48824, USA*
[3] *Department of Chemistry, Michigan State University, East Lansing, MI 48824, USA*
[4] *Department of Physics, Hope College, Holland, MI 49422-9000, USA*
[5] *Department of Physics, Central Michigan University, Mount Pleasant, MI 48859, USA*
[6] *Department of Physics and Astronomy, Augustana College, Rock Island, IL 61201, USA*
[7] *Department of Physics and Astronomy, Ohio Wesleyan University, Delaware, OH 43015, USA*
[8] *Department of Physics, Concordia College, Moorhead, MN 56562, USA*
[9] *Department of Physics, Gettysburg College, Gettysburg, PA 17325, USA*

(Dated: March 31, 2015)

A previously published measurement of the reaction of a 59 MeV/nucleon ^{14}Be beam on a deuterated polyethylene target was further analyzed to search for ^{12}He as well as initial state effects in the population of the ^{10}He ground state. No evidence for either was found. A lower limit of about 1 MeV was determined for a possible resonance in ^{12}He. In addition, the 3-body decay energy spectrum of ^{10}He could not be described by a reaction mechanism calculation based on the halo structure of the initial ^{14}Be assuming a direct α-particle removal reaction.

PACS numbers: 21.10.Dr, 25.60.-t,27.20.+n, 29.30.Hs

I. INTRODUCTION

Our recent measurement of the ^{10}He ground state [1] did not support the theoretical explanation for the difference in resonance energy observed in two types of reactions [2]. While a missing mass measurement at Dubna using a (t, p) reaction had reported the ground state to be at 2.1(2) MeV [3], a one-proton removal reaction at GSI from a high-energy ^{11}Li beam found the ground state to be at a lower energy of 1.54(11) MeV [4]. Subsequently, Grigorenko and Zhukov showed that the observed peak in the 3-body spectrum of the GSI invariant mass measurement could result from the halo nature of the ^{11}Li projectile [2], apparently reconciling the descrepancy between the GSI and Dubna results.

In our experiment we populated ^{10}He in the two-proton and two neutron removal reaction from a ^{14}Be beam at an energy of 59 MeV/nucleon. This reaction was considered to be more dissipative than the one-proton removal reaction and thus the invariant mass spectrum should not be influenced by the proposed initial state effects. We measured a resonance energy of 1.60(25) MeV [1] consistent with the GSI results [4] but in disagreement with the Dubna data [3].

Earlier this year Sharov *et al.* [5] suggested that our results could be explained by assuming that ^{10}He was populated directly by an α-cluster removal, thus again exhibiting a structure which is due to the halo-nature of the initial ^{14}Be.

In the present paper, we report a more-detailed analysis of the data to investigate possible evidence for direct cluster removal and search for a resonance in ^{12}He.

II. EXPERIMENTAL METHOD

The experiment was performed at the National Superconducting Cyclotron Laboratory (NSCL) where a 3196 mg/cm^2 ^{9}Be target was bombarded with ^{18}O at 120 MeV/nucleon. The A1900 fragment separator allowed for selection of ^{14}Be from the other fragmentation products as well as the primary beam. The secondary beam then impinged on a 435 mg/cm^2 deuterated polyethylene target at a rate of approximately 1000 pps. The resulting charged fragments were bent by a 4 Tm superconducting Sweeper Magnet [6] into a collection of position and energy sensitive charged-particle detectors, which allowed for element identification of helium via a ΔE − E measurement. Isotope identification of ^{8}He was achieved through correlations between time-of-flight, dispersive angle, and dispersive position of the fragments. This technique is described in further detail in Ref.[7]. The neutrons emitted in-flight traveled undisturbed by the magnetic field towards MoNA (Modular Neutron Array) [8], which provided a measurement of position and time-of-flight. Together, MoNA and the Sweeper system provide a full kinematic measurement of the neutrons and the charged fragment, from which the decay energies of $^{9-12}$He can be calculated. Additional experimental details can be found in Refs. [1, 9].

* jonesm@nscl.msu.edu
† Present Address: TRIUMF, 4004, Wesbrook Mall, Vancouver, British Columbia, V6T 2A3 Canada
‡ Present Address: LANL, Los Alamos, New Mexico 87545. USA

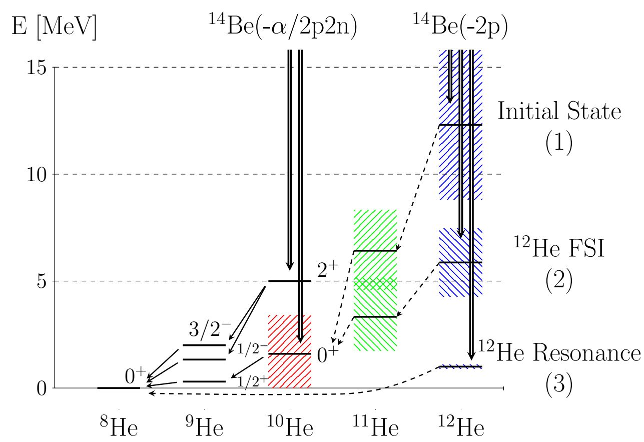

FIG. 1. (Color online) Level scheme for the population and decay of ^{10}He from α/2p2n or 2p removal. Hatched areas indicate approximate widths.The different scenarios for populating ^{12}He are described in section III b.

III. ANALYSIS

In the initial analysis [1] only the 3-body decay energy spectrum of ^{10}He in coincidence with two neutrons was calculated. However, a direct two-proton removal reaction would populate ^{12}He which then would emit four neutrons in-flight in coincidence with ^{8}He. A potential resonance in ^{12}He could be observable in the 5-body decay energy spectrum. Thus, we extended our analysis to N-body decay energy spectra for $2 \leq N \leq 5$ corresponding to the decays of $^{9-12}$He. The N-body decay energy is defined as $E_{\mathrm{decay}} = M_{\mathrm{Nbody}} - M_{^{8}\mathrm{He}} - \sum_{i=1}^{i=N-1} m_{\mathrm{n}}$, where $\mathrm{M_{Nbody}}$ is the invariant mass of the N-body system, $\mathrm{M}_{^{8}\mathrm{He}}$ the mass of ^{8}He, and m_{n} the mass of a neutron. The invariant mass for an N-body system was calculated from the experimentally measured four-momenta of ^{8}He and the first $N-1$ time-ordered interactions in MoNA.

Due to multiple scattering events in the array, it is necessary to discriminate between true and false multi-neutron events. For 1-neutron events, the contribution from ^{9}He can be enhanced by gating on multiplicity = 1 events. In the case of ^{10}He (2n events) separation of scattered events from real two-neutron events was accomplished by applying causality cuts on the relative distance and velocity between the first two interactions in MoNA as described in [1].

Ideally, similar cuts should be applied to the 4-body and 5-body decay energy spectra. However, there were insufficient counts for these cuts to be applied. No resonances are apparent in these spectra which are dominated by multiple scattering events. It was estimated by simulation that the fraction of true 4 neutron events in the 5-body spectra is approximately 8% below 1 MeV, and 3% above 1 MeV.

The large number of free parameters makes it difficult to take all possible population and decay paths for forming ^{8}He from ^{14}Be into account. Thus, the simulations were limited to direct population of ^{12}He and ^{10}He. Three different scenarios, described later, were considered separately for the population of ^{12}He. For ^{10}He the population of the 0^{+} ground state and the 2^{+} first excited states were included. The simulations did not distinguish between α-removal or 2p2n removal. However, a larger contribution to the spectra relative to the ^{12}He population would indicate an α removal as the 2p2n removal cross section is expected to be significantly smaller than the 2p removal cross section. The different population paths and subsequent decays included in the simulation are shown in Figure 1.

The removal reactions were modeled with the Goldhaber reaction model in conjunction with a detailed Monte-Carlo package. These simulations included the beam characteristics, the reaction mechanism, and the subsequent decay. Using GEANT4 [10] and MENATE_R [11], the efficiency, resolution, and acceptances of MoNA and the charged particle detectors following the dipole Sweeper magnet were incorporated into the simulations, making the results directly comparable to experiment. It has been shown that the inclusion of MENATE_R is important for properly simulating the response of plastic scintillators [12].

The key distinguishing feature between α/2p2n-removal and 2p removal is the total number of neutrons emitted in each reaction. Hence, it is important to consider both the one and two-neutron decay energy spectra in addition to the multiplicity distribution. This is done by a simultaneous χ^2 minimization procedure on the following six experimental spectra found in Figure 2: (a) the ^{8}He + 1n decay energy, (b) the multiplicity = 1 gated ^{8}He + 1n decay energy, (c) the ^{8}He + 2n decay energy, (d) the decay energy of ^{8}He + 2n gated on multiplicity = 2, (e) the ^{8}He+2n decay energy with the causality cut, and finally (f) the multiplicity distribution.

This simultaneous minimization adds additional constraints to the final fit results compared to fitting the two- and three-body decay energy spectra separately to extract the ^{9}He and ^{10}He resonance parameters, respectively.

A. Direct α/2p2n Removal

Due to large uncertainties in ^{10}He and the ^{9}He subsystem, we first consider only direct population of ^{10}He, or 2n events. Here we assume that ^{10}He is populated exclusively through α or 2p2n removal, and that ^{9}He is populated only by sequential decay as shown in Fig. 1. The sequential emission is modelled following the formalism of Volya et al. [13]. We consider both the decay of the ground (0^{+}) and first excited (2^{+}) state of ^{10}He through three states in ^{9}He: the $1/2^{+}$, $1/2^{-}$, and $3/2^{-}$ states. The $1/2^{-}$ state was fixed in energy and width at E = 1.33 MeV, Γ = 0.1 MeV [4]. Additionally, the widths of the $1/2^{+}$ and $3/2^{-}$ states were fixed at 8.4 MeV

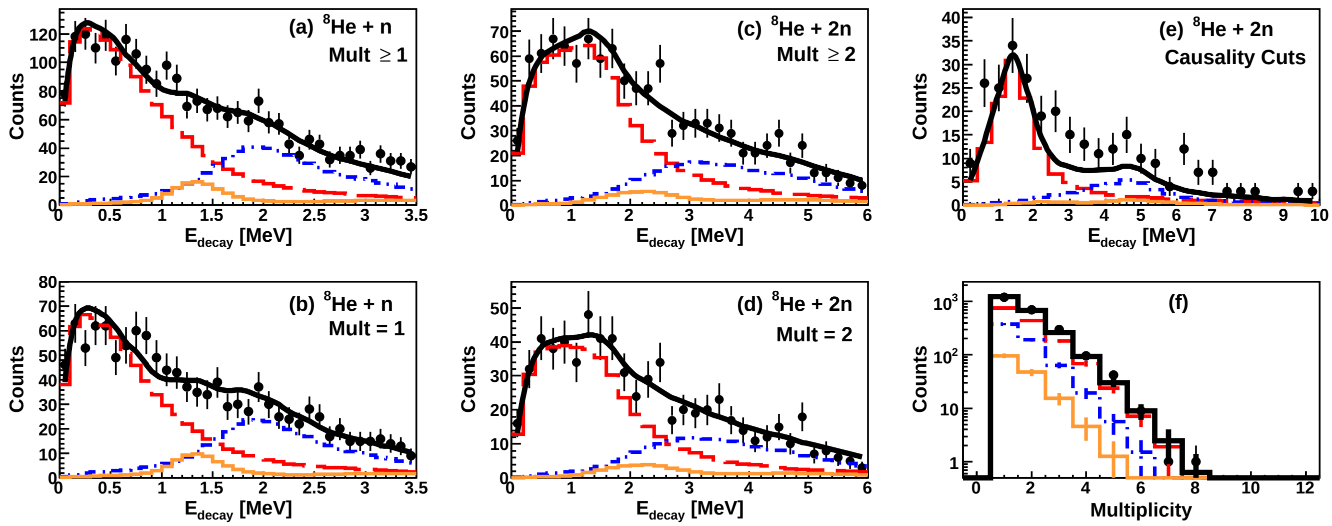

FIG. 2. (Color online) Decay energy spectra assuming α/2p2n-removal for (a) ^{8}He + 1n , (b) ^{8}He + 1n gated on multiplicity = 1, (c) ^{8}He + 2n, (d) ^{8}He + 2n gated on multiplicity = 2, (e) ^{8}He + 2n with causality cuts, and (f) the multiplicity distribution. Measured spectra are indicated by black solid circles. The best fit for α or 2p2n removal with no contribution from 2p removal is shown as solid black. The fit parameters can be found in Table 1. The $l = 0$ sequential decay from the 0^+ ground state in ^{10}He is shown by the dashed/red histogram while the dot-dash/blue and solid/orange histograms are decays from the 2^+ state to the $3/2^-$ and $1/2^-$ states in ^{9}He, respectively.

and 0.7 MeV [4, 14], respectively, but allowed to vary in energy. For ^{10}He, both states were allowed to vary in energy. However, the width of the 2^+ was restricted to 1.64 MeV[4]. The range of energies was chosen to encompass a variety of previous measurements [3, 4, 14–23]. While it is possible to include a decay through the $5/2^+$ state in ^{9}He at energies reported from previous experiments [14, 15], this resonance is not well-resolved in the data, of higher energy, and is thus excluded from this analysis. The dominant components needed to describe the data are the decay of the 0^+ state in ^{10}He through the $1/2^+$ state in ^{9}He, and the decay of the first-excited 2^+ though the $1/2^-$ and $3/2^-$ states.

The fitting results with the assumption of α/2p2n-removal are shown in Fig.2. With a χ^2 of 161 for 152 degrees of freedom, the model shows good agreement with the data and with previous experiments. The resonance parameters for the best fit are summarized in Table 1. Only two states differed in energy compared to previous measurements. The $3/2^-$ state in ^{9}He tended to be slightly lower at $1.9^{+0.4}_{-0.2}$ MeV, in contrast to 2.4 MeV [14], and the minimum χ^2 suggests a value of $4.7^{+0.8}_{-0.5}$ MeV for the 2^+, compared to 4.0 MeV [4]. It should be mentioned that the fit is insensitive to certain parameters, namely the scattering length in ^{9}He and, in general, resonance widths. For example, scattering lengths down to −10 fm for the $1/2^+$ state in ^{9}He and widths of the 0^+ larger than 1 MeV resulted in equally good fits. More importantly, however, the fit demonstrates that it is possible to describe the data entirely with two-neutron events using values in agreement with previous experiments. There is an underprediction of events in the 3-body decay energy

TABLE I. Resonance parameters for states in ^{9}He and ^{10}He used to fit the 1n and 2n decay energy spectra. Values with a dagger indicate they were adjusted to best describe the data.

Nucleus	J$^\pi$	E [MeV]	Γ [MeV]
^{9}He	$1/2^+$	-3 fm[a] [4]	8.4 [4]
	$1/2^-$	1.33 [4, 14]	0.1 [14]
	$3/2^-$	$1.9^{+0.4\dagger}_{-0.2}$	0.7 [14]
^{10}He	0^+	1.6 [1]	1.8 [1]
	2^+	$4.7^{+0.8\dagger}_{-0.5}$	1.64[4]

[a] Scattering length for $l = 0$ state

with causality cuts (panel 5 in Fig. 2), but this discrepancy is not enough to reject the fit when the other histograms are considered. Increasing the widths of the states in ^{10}He, or changing their energies affects their shape in the ^{9}He spectra, and the fit presented is the best simultaneous fit. Thus the data do not require significant contributions from direct two-proton removal, which would be expected to have a large cross section compared to α or 2p2n removal. However, it is still possible for a component from 2p-removal to be present up to a limit given by statistical uncertainty.

B. Two-proton Removal

In order to determine any possible contributions from direct population of ^{12}He by two-proton removal we modelled the decay of ^{12}He → ^{8}He + 4n. The three different cases for the population of ^{12}He were (1) a distribution in-

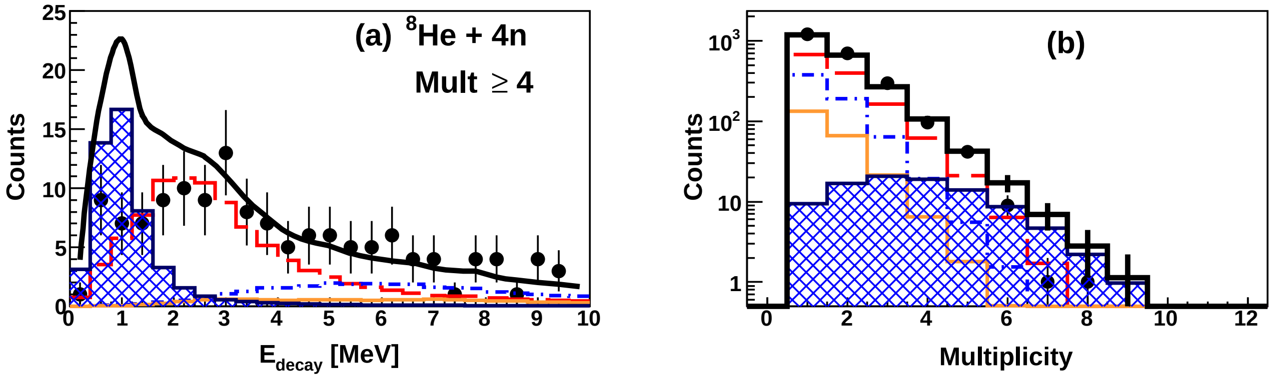

FIG. 3. (Color online) 5-body decay energy spectra for ^{8}He + 4n for all multiplicities (left), and neutron multiplicity distribution (right). The hatched blue histogram is the contribution from a 5-body breakup of ^{12}He at E = 1 MeV, Γ = 100 keV with R(4n/2n) = 1.5%. The dash, dot-dashed, and solid lines are the same as in Figure 2.

fluenced by the initial halo structure of ^{14}Be, henceforth refered to as the ^{14}Be Inital State Structure (ISS)[24], (2) a resonant Final-State Interaction (^{12}He FSI)[24] peaking at $\sim$ 6.5 MeV, and (3) a low-lying resonance described by a Breit-Wigner centered at $\sim$ 1 MeV. In the ISS and FSI cases, it was assumed that ^{12}He decayed to the 0^{+} ^{10}He ground state with a phase space distribution [25], where the 3-body decay energy is determined by the difference between the ^{10}He and ^{12}He decay energy distributions. The remaining ^{10}He then decayed sequentially through ^{9}He following the paths described previously. The third case was modeled as a 5-body phase-space break-up decaying directly to ^{8}He. The 2p-removal decay paths are shown in Fig. 1.

The minimization method described previously was expanded to include two additional spectra to search for a 4n component. In order to enhance the sensitivity to 4n events, the raw 5-body decay energy spectrum and the 5-body decay energy spectrum gated on multiplicity $\geq$ 4 were analyzed. Although the statistics of these 5-body spectra are small and contain very few real 4-neutron events they still provide a measure of the amount of scattering in the array. If the reaction were to proceed predominantly by 4n emission, the 5-body spectra constructed from the first 4 hits will be enhanced, especially for low energy neutrons. Combined with the multiplicity distribution, these spectra provide sensitivity to the number of neutrons emitted in the reaction.

In the minimization procedure we start from the α/2p2n-description, and minimize χ^2 on the same six experimental histograms as before. However, we also track the log-likelihood ratio, Ln[λ], of two 5-body spectra,^{8}He + 4n, and ^{8}He + 4n gated on multiplicity = 4, as well as the multiplicity distribution. The $n\sigma$ confidence intervals are determined by $-\Delta\mathrm{Ln}[\lambda] \approx \Delta\chi^2(k)/2$, where $\Delta\chi^2(k)$ is the corresponding deviation from the minimum required to integrate 68%, 95%, and 99% of a χ^2 distribution with k degrees of freedom. Each component of the fit was allowed to vary independently, and was treated as a degree of freedom. We choose to track the fit-quality

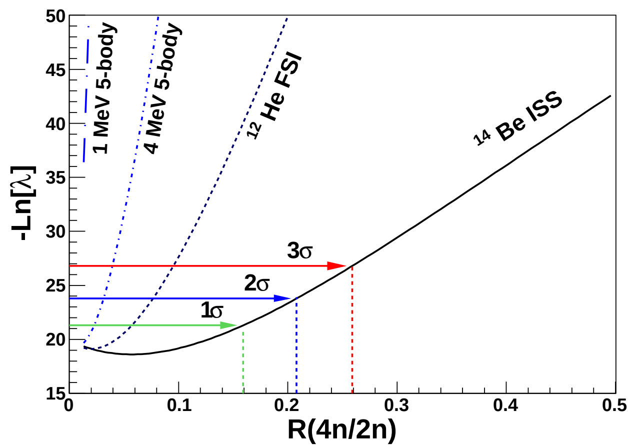

FIG. 4. (Color online) Maximum likelihood for the 5-body decay spectra and multiplicity as a function of the ratio of 2p to α or 2p2n removal R(4n/2n) for several possibilities in the ^{12}He system: A 1 MeV resonance (long-dash-dot/blue), a 4 MeV resonance (short-dash-dot/blue), a ^{12}He FSI calculation (dotted/black) and the ISS calculation (solid). The 1σ, 2σ, and 3σ confidence levels are shown by the green, blue, and red arrows respectively.

of the 5-body spectra because they are most sensitive to the presence of a 4n component from 2p removal.

We then examine the ratio of 4n to 2n amplitudes, R(4n/2n) or 2p to α/2p2n-removal cross sections. Taking the minimized parameters from the α/2p2n fit, the amplitude of the 2p component is gradually increased while the remaining α/2p2n-components are re-minimized on the six histograms mentioned earlier. This procedure adjusts R(4n/2n) to best describe the decay energies and relative ratios of events while allowing one to track the increasing deviation from the 5-body spectra and the multiplicity.

Overall the best fits achieved for these scenarios are similar to the fits shown in Figure 2 and are not shown separately. Not surprisingly, since the data can be described with α/2p2n-removal alone, the contribution

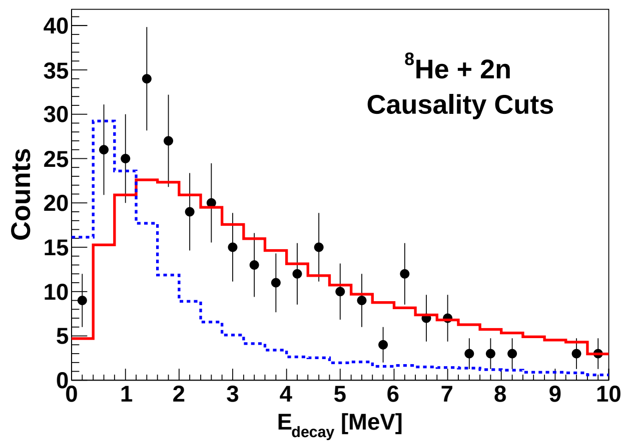

FIG. 5. (Color online) Calculated 3-body spectrum with causality cuts for ^{8}He + 2n under the assumption of α-removal based on the halo structure of the initial ^{14}Be (solid/red). The same distribution after folding with experimental resolution, efficiency and acceptances is shown in dashed/blue.

from 2p removal in the present fits is small. It should be mentioned that populating ^{10}He from 2p removal without any α/2p2n contribution does not describe the data well.

Figure 3 shows the results of a calculation assuming a resonance in ^{12}He at 1 MeV populated with a strength of only 1.5% that of the net α/2p2n components. In the 5-body decay energy spectrum (left panel) a large excess of events relative to the data is evident around 1 MeV. At the same time the multiplicity distribution (right panel) is overpredicted for multiplicities beyond 6. Since one would expect the presence of a distinct resonance in ^{12}He to be strongly populated in the 2p removal reaction from ^{14}Be, the data do not show evidence of a low-lying state in ^{12}He below 1 MeV.

Even for the other scenarios, which do not assume a distinct resonance in ^{12}He, the upper limit for their population is low. Figure 4 shows the log-likelihood as a function of R(4n/2n) for several cases. In no case does the ratio exceed about 30% and remain within 3σ confidence. The figure demonstrates that the upper limit of R(4n/2n) increases with excitation energy of the 5-body system. While the energy for the ^{12}He resonance calculation is at 1 MeV (long-dash-dot/blue), and 4 MeV (short-dash-dot/blue) the mean excitation energies for the FSI calculation (dotted/black) and the ISS calculation (solid) are at about 6.5 MeV and 12 MeV, respectively. This increase in the upper limit of R(4n/2n) is predominantly due to the drop-off in efficiency for higher decay energies.

IV. DISCUSSION

A small value of R(4n/2n) indicates a direct population of ^{10}He. Since the cross section for 2p2n removal is estimated to be at least an order of magnitude smaller than the 2p removal reaction [26, 27] we consider the possibility of α removal. This process was proposed in Ref. [5] in order to explain our decay energy spectrum. In addition, α removal has also been suggested to explain the population of ^{12}Be from a 55 MeV/nucleon ^{17}C beam incident on a beryllium target [26]. The α-removal 3-body distribution for ^{10}He was derived from the same model used to explain the removal from ^{11}Li as presented in Ref. [5]. In this model ^{14}Be is treated as a ^{12}Be core and two neutrons, with the ^{12}Be core considered as ^{8}He + α. Figure 13 of Ref. [5] showed that such a calculation describes the 3-body decay energy from our experiment well. However, the calculations had not been folded with experimental resolutions and efficiencies. The shape of the calculated distribution is significantly changed once the experimental conditions are applied as shown in Figure 5. The peak of the distribution is shifted towards lower decay energies and the overall width is narrower. Adding a 4n component from the models discussed here does not account for the difference, as the increased 4n contribution overpredicts the multiplicity distribution.

One potential explanation for the small contribution of 2p removal events as well as the discrepancy between the data and the direct α-removal model of the 3-body decay energy spectrum might be the fact that the charged ^{8}He fragments were not detected at the peak of their momentum distribution. The Sweeper magnet was set for lower rigidities so that only the low-energy tail of the overall distribution was recorded. These events probably originate from the more dissipative reactions which could bias the data towards α/2p2n removal relative to 2p removal. A similar suppression of the 2p removal cross-section was observed in the breakup of ^{17}C, where also only the low-energy tail of the momentum distribution was measured [26].

It is possible that the more dissipative reactions could have reduced the effect of the correlation from the ^{14}Be initial state for the direct α removal. In that case then, the observed resonance in ^{10}He should have agreed with the higher value of about 2 MeV previously reported from transfer measurements. Nevertheless, such a dependence of the decay energy spectra on the fragment momentum distribution has not been observed in the past in similar reactions.

In summary, a complete inclusive analysis of multi-neutron decay energy spectra is a tool to explore neutron unbound systems which decay via the emission of three or four neutrons even if the statistics are not sufficient to extract spectra with clean identification of each neutron. In the present case, no evidence for the existence of a low-lying ($\leq$ 1 MeV) resonance in ^{12}He was found. The 3-body decay energy spectrum of ^{10}He could not be described by a reaction mechanism calculation based on the halo structure of the initial ^{14}Be assuming a direct α-particle removal reaction. In order to distinguish direct α removal from 2p2n removal it will be necessary to measure coincident α particles in addition to the charged fragment and the neutrons.

ACKNOWLEDGMENTS

We would like to thank L.V. Grigorenko for thoughtful discussion, and for providing theoretical estimates of the 5-body decay energies of the ^{12}He system. This work was supported by the National Science Foundation under Grants No. PHY09-22335, PHY09-69058, PHY09-69173, PHY12-05357, PHY12-05537, and No. PHY11-02511. The material is also based upon work supported by the Department of Energy National Nuclear Security Administration under Award No. DE-NA0000979.

[1] Z. Kohley *et al.*, Phys. Rev. Lett. **109**, 232501 (2012).
[2] L. V. Grigorenko and M. V. Zhukov, Phys. Rev. C **77**, 034611 (2008).
[3] S. Sidorchuk *et al.*, Phys. Rev. Lett. **108**, 202502 (2012).
[4] H. Johansson *et al.*, Nucl. Phys. A **842**, 15 (2010).
[5] P. G. Sharov, I. A. Egorova, and L. V. Grigorenko, Phys. Rev. C **90**, 024610 (2014).
[6] M. Bird *et al.*, IEEE Trans. Appl. Supercond. **15**, 1252 (2005).
[7] G. Christian *et al.*, Phys. Rev. C **85**, 034327 (2012).
[8] B. Luther *et al.*, Nucl. Instrum. Methods A **505**, 33 (2003).
[9] J. Snyder *et al.*, Phys. Rev. C **88**, 031303(R) (2013).
[10] S. Agostinelli *et al.*, Nucl. Instrum. Mehtods A **506**, 240 (2003).
[11] B. Roeder, EURISOL Design Study, Report No. 10-25-2008-006-In-beamvalidations.pdf , pp. 3144 (2008).
[12] Z. Kohley *et al.*, Nucl. Instrum. Methods A **682**, 59 (2012).
[13] A. Volya, EPJ Web of Conferences **38**, 03003 (2012).
[14] H. Bohlen *et al.*, Prog. Part. Nucl. Phys. **42**, 17 (1999).
[15] T. Al Kalanee *et al.*, Phys. Rev. C **88**, 034301 (2013).
[16] L. Chen *et al.*, Phys. Lett. B **505**, 21 (2001).
[17] K. Seth *et al.*, Phys. Rev. Lett. **58**, 1930 (1987).
[18] K. Seth, Nucl. Phys. A **434**, 287 (1985).
[19] W. von Oertzen *et al.*, Nucl. Phys. A **588**, 129 (1995).
[20] G. Rogachev *et al.*, Phys. Rev. C **67**, 041603 (2003).
[21] M. S. Golovkov *et al.*, Phys. Rev. C **76**, 021605 (2007).
[22] M. S. Golovkov *et al.*, Phys. Lett. B **672**, 22 (2009).
[23] A. Matta *et al.*, RIKEN Accel. Prog. Rep. **45** (2012).
[24] L. V. Grigorenko, private communication (2014).
[25] F. James, Monte Carlo Phase Space, CERN **68-16** (1968).
[26] A. N. Kuchera *et al.*, Phys. Rev. C **91**, 017304 (2015).
[27] J. A. Tostevin, private communication (2014).